PRACTICAL ISSUES IN THE LOCATION OF SMALL EVENTS UNDER A CTBT: POOR STATION COVERAGE AND POORLY KNOWN VELOCITY STRUCTURE

Katharine Kadinsky-Cade, Rong-Song Jih, Anton Dainty and John Cipar
Earth Sciences Division (PL/GPE)
Phillips Laboratory
29 Randolph Rd
Hanscom AFB, MA 01731

Phillips Laboratory Task # 76000908

ABSTRACT

In regions that do not contain good station coverage, a reasonably well known velocity structure and moderate or large magnitude events (the latter needed for calibration using teleseismic constraints on the location of a master event), it is very difficult to obtain accurate regional event locations. In this situation standard error ellipses generated during event locations may give the impression that an event location is better determined than it really is. False interpretations of the data may be due to a three dimensional velocity structure bias unaccounted for by the method, or simply to phase misidentification. Forward waveform modeling does help constrain the structure, however this approach contains a number of pitfalls. Modeling works best if ground truth is available at several epicentral distances and azimuths. Otherwise an inappropriate model might be constructed by matching synthetic waveforms and arrival times to observed data assumed to be at the wrong location. That model might thereafter be used to locate additional events. Regional arrays, or arrays originally constructed for teleseismic monitoring, can sometimes be used to identify regional phases using frequency-wavenumber (F-K) measurements of phase velocity in short (3-5 second) windows on the seismograms, however this only gives a solution if the signal to noise ratio is high. The F-K method is sensitive to the chosen center frequency and bandwidth, and to three dimensional heterogeneities surrounding the array. Some of these practical issues are discussed in scenarios involving events located within 500 km of a recording station or array. We model seismograms using reflectivity and linear finite difference techniques, assuming flat isotropic layers for simplicity. Phases that can be identified and modeled at these distances include P and S wave reflections and refractions. The Lg phase cannot be used as a phase with fixed group velocity throughout this distance range. This study highlights the importance of developing regional velocity structures for the crust and upper mantle that are well constrained by controlled source experiments.

Key words: phase identification, event location, crustal velocity structure, waveform modeling

OBJECTIVES:

Our objectives are to (1) provide practical solutions to the problem of seismic phase identification in a region sparsely populated by seismic stations, and (2) use these phases to locate seismic events at regional distances. The underlying scientific problem is how to determine an appropriate velocity structure for a region in the absence of ground truth or large well constrained sources that have been located teleseismically.

RESEARCH ACCOMPLISHED:

We consider a generic region in which small infrequent events occur. These might typically be earthquakes or explosions related to mining activity. We assume that only one station or array has recorded these events due to their size. That station or array is situated within 500 km of the sources under study, therefore the crust and upper mantle structure have a strong effect on wave propagation. The question in a CTBT might then be to determine where a specific event X in that region is really located.

The problem is that we do not know the velocity structure in this region. Because of the poor station coverage we cannot perform a joint inversion to reliably obtain velocity structure and event locations, as has been done by Crosson (1976) or by Goins et al. (1981).

If the locations and origin times of the events that have been recorded at the station or array are only approximate, we cannot determine a velocity structure by simply fitting observed phase arrival times with theoretical travel time curves as one would do in a controlled source refraction experiment. Fitting S-P times is not practical either, because seismograms plotted on a travel time (t) versus distance (x) curve are free to move in both the t and x directions due to the unconstrained hypocenter and origin time. If the hypocenter of one of the events is known independently, but the origin time is not precisely known, that event can be used to help construct a travel time curve. In that case the S-P time provides a useful modeling constraint because the position of the seismogram along the distance axis is fixed.

It is possible to assume a starting model for the crust and upper mantle in the region by borrowing a model from another better studied region with similar tectonic characteristics. Continental crust and upper mantle structures have been obtained in a variety of regions around the world (Christensen and Mooney, 1995), and it is often possible to find a reasonable starting structure by analogy with another region. Alternatively, one can determine a starting model using surface waves that have crossed the region under study. Once a starting model has been determined, the whole suite of regional events can be relocated based on that model. Geologically reasonable end-member models can be tested to search for some measure of confidence that includes the effect of the velocity structure. If we perform a joint (relative) relocation of all events using multiple P and S arrivals , the smallest RMS error should correspond to the best of the velocity models considered.

Figure 1 is a set of regional events that have occurred in some arbitrary area. These events can be plotted in record section format only because some crustal structure has been selected and the events have been located accordingly. The lineup of the P and S arrivals gives the impression that the structure can be extracted from this plot by superimposing travel time curves on the plot. However the lineup of the phases has been artificially imposed by the assumption of a specific velocity structure. Other structures and resulting locations will give new positions for the seismograms on the plot and result in phase lineups as well. Ideally some independent information ("ground truth") will help in the selection of the best velocity structure.

In Figure 2 we have plotted synthetic seismograms and travel time curves for two models. The travel time curves constructed here by ray tracing assume a spherically symmetric homogeneous earth. The one dimensional ray tracing code handles gradients, and is based on Bullen's (1976) treatment of seismic rays in a spherically stratified earth model. We have chosen a surface source, and include direct rays, refracted rays and simple reflections off the Conrad discontinuity and the Moho. We have not plotted phase conversions such as PS or PmS in the travel time curves; they are included in the synthetic seismograms. Model A is composed of the upper few hundred kilometers of the IASP91 earth model (Kennett, 1991; Kennett and Engdahl, 1991). Kennett discussed the limitations of this model recently (Kennett, 1995), pointing out that IASP91 is a convenient hybrid model, but that it was constructed in part by incorporating some artificial constraints. Furthermore it is based on data from a number of different regions, and may not be appropriate for the region under study. The IASP91 model is characterized by a simple two layer crust over an upper mantle with a very weak positive gradient. Model B is generated by replacing the 2 layer crust in the IASP91 model by a 4 layer crust that is more like a crust in a continental shield area. The additional layers add to the complexity of the travel time curve. Another model to test might be a continental shield-type crust overlying a corresponding shield-type mantle. The travel time curves only provide expected arrival times for comparison with the data.

To incorporate amplitude information we turn to waveform modeling. The velocity structure can have a strong effect on amplitudes. For example a strong velocity gradient at the Moho can boost up the amplitudes of the Pn and Sn phases. An appropriate value for Q must be determined as well. Qp and Qs can be determined by trial and error, or by independent spectral or coda decay studies. For each model we construct synthetic seismograms using the linear finite difference and reflectivity methods. The reflectivity code was provided by Harley Benz of the U.S. Geological Survey (Fuchs and Müller, 1971; Benz et al., 1990). The linear finite difference code we use was originally developed at Teledyne Geotech's Alexandria Laboratory (cf. Jih, 1993), and has been modified to include a prototype attenuation operator currently being tested at Phillips Laboratory. In both cases we use an explosion source at the surface. After performing the computation of displacement seismograms we differentiate to get velocity records and apply a high pass filter to simulate short period seismograms. All calculations are done on a Sun Microsystems SPARC20 workstation. Finite difference results are shown in Figure 2. The finite difference calculation is computationally intensive and currently only practical out to 250 km distance for the frequency band of interest. In Figure 3 we have carried the reflectivity calculation out to 500 km for the second model. To avoid instabilities and speed up the calculation we have provided an upper frequency limit of 2 Hz in Figure 5. This simplifies the appearance of the seismograms to some extent. Even with this frequency limitation it is useful to compute seismograms out to 500 km because the 350-500 km distance range helps us constrain the velocity structure of the upper mantle.

If array data are available we can determine apparent velocities of regional phases using frequency-wavenumber (F-K) spectral analysis. Unfortunately it appears that there are some problems inherent in this approach, most likely related to heterogeneity of the crust and resulting frequency dependence of scattering. An example is shown in Figures 4a-4b. This event is a quarry blast from Blåsjø Quarry, recorded at the NORESS array (see Dainty and Toksöz, 1990 for more information). In this case the distance and azimuth of the quarry are known (324 km, 243°; location from Dysart and Pulli, 1987). We have selected two subsets of array stations. Rather than making use of the full complement of NORESS stations we are decimating the array, to see if an array with spacing more appropriate for teleseismic monitoring can effectively see the seismic wavefield decomposed into plane waves at regional distances. We seem to get strong apparently stable spectral peaks, but the phase velocities measured at two different frequencies are quite different from each other. Neither set approximates values expected for a reasonable flat layered structure. We start by selecting 6 array stations, with approximately 2 km spacing between stations, and a center frequency of 1 Hz and bandwith $\pm 10\%$. Next we select 13 stations with approximately 1 km between stations, and a center frequency of 2

Hz. We should get the same result as in the first case. Instead we find inconsistencies in the phase velocities determined using the different frequency bands. The phase velocities we would expect, based on an IASP91 crust, are Pn-8.1 km/sec, P*-6.5 km/sec, PmP-6.6 Km/sec, Pg-5.8 km/sec, Sn-4.5 km/sec, SmS-3.8 km/sec. If we assume a crustal model such as that of Kanestrom and Haugland (1971), as described by Vogfjord and Langston (1990), we expect slightly higher phase velocities. Here, for example, we should find Pn-8.2 km/sec, PmP-7.3 km/sec, Sn-4.8 km/sec, SmS-4.2 km/sec. We see that the F-K plots give unreasonable results for the first P arrival (Pn) at both frequencies, and questionable results for other phases. Note that the SmS velocity is getting low enough that the corresponding wavenumber is at the borderline of being acceptable for analysis with these values of station spacing, due to possible aliasing.

RECOMMENDATIONS AND FUTURE PLANS

It is clear from the above examples that a combination of raytracing and waveform modeling can be an effective way to characterize regions with few events and fewer stations. It must however be emphasized that waveform modeling without ground truth is subject to misinterpretation. One important factor is the misidentification of phases. This has been mentioned by Vogfjord and Langston (1990). Phases may be missed because they have low amplitude, or mislabeled because of simplified assumptions. For example at short distances (less than 150-200 km) Lg is not a phase with a constant group velocity of 3.5 km/sec. One can instead look for the SmS phase, which can be quite strong and which comprises the beginning of the Lg wavetrain at greater distances. The second factor is the bias provided by the crust and upper mantle. This can be due to anisotropy or to three dimensional effects. For example one factor that may contribute to the difficulty in determining reasonable phase velocities for the Blåsjø Quarry event mentioned above is the presence of the Oslo Graben southwest of the NORESS array (see graben location in Vogfjord and Langston, 1990).

Further work is required to quantify the effects of geologically realistic heterogeneities on travel times and amplitudes. The ability to do rapid relocations using a variety of velocity models through a range of near to far regional distances is important, and we are now focusing our efforts in this area. We are basing our travel time calculations on the tau-p method of Buland and Chapman (1993), for which computation is rapid. If we do not have detailed independent velocity information in an area it seems reasonable to work with a starting one-dimensional crustal model, and quantify how variations in that model would affect our locations. It seems clear that a simple global model like IASP91 is unlikely to be sufficient in specific regions for waveform modeling and reliable locations within a 500 km range.

Use of arrays for regional phase velocity determinations is problematic. Previous work at NORSAR has suggested that P and S energy can be differentiated on F-K plots at NORESS, but that it may sometimes be difficult to separate out phases more precisely from inferred phase velocities (Mykkeltveit and Bungum, 1984; Mykkeltveit et al., 1990). It may be that calibration of each array is necessary as a function of distance and frequency. This is clearly not appropriate in the situation described here in which little if any ground truth is presumed available, and in which we would like to use arrays to constrain crustal structure and identify specific P and S arrivals within the context of that structure.

REFERENCES:

Benz, H., R. Smith and W. Mooney, 1990, Crustal structure of the Northwestern Basin and Range Province from the 1986 PASSCAL seismic experiment, *Jour. Geophys. Res., 95*, pp. 21,823-21,842.

Buland, R. and C. Chapman, 1983, The computation of seismic travel times, *Bull. Seis. Soc. Am., 73*, pp. 1271-1303.

Bullen, K.E., 1976, An introduction to the theory of seismology, Third Edition, Cambridge University Press, Cambridge, U.K., 381 pp.

Christensen, N.I. and W.D. Mooney, 1995, Seismic velocity structure and composition of the continental crust: a global view, *Jour. Geophys. Res.,* 100, 9761-9788.

Crosson, R., 1976, Crustal structure modeling of earthquake data 1. Simultaneous least squares estimation of hypocenter and velocity parameters, *Jour. Geophys. Res., 81*, 3036-3046.

Dainty, A.M. and M.N. Toksöz, 1990, Array analysis and seismic scattering, *Bull. Seis. Soc. Am., 80*, 2242-2260.

Dysart, P.S. and J.J. Pulli, 1987, Spectral study of regional earthquakes and chemical explosions recorded at the NORESS array, in Tech. Rep. for the Period 1 April-30 June 1987, *Tech. Rep. C87-03*, Center for Seismic Studies, Arlington, VA, pp 3-21 - 3-24.

Fuchs, K. and G. Müller, 1971, Computation of synthetic seismograms with the reflectivity method and comparison with observations, *Geophys. J. Roy. Astron. Soc., 23*, 417-433.

Goins, N.R., A.M. Dainty, and M.N. Toksöz, 1981, Lunar seismology: the internal structure of the moon, *Jour. Geophys. Res., 86*, 5061-5074.

Jih, R.-S., 1993, User's manual of FD2: a software package for modeling seismological problems with 2-dimensional linear finite-difference method, *Special Topical Report TGAL-93-06*, Teledyne Geotech, Alexandria, VA.

Kanestrom, R. and K. Haugland, 1971, Profile section 3-4 in Deep Seismic Sounding in Europe, A. Vogel, Editor, Swedish Natural Science Research Council, Stockholm, Sweden,76-91.

Kennett, B.L.N.(editor), 1991, IASPEI 1991 Seismological Tables, Research School of Earth Sciences, Australian National University, 167 pp.

Kennett, B.L.N., 1995, The underdetermined earth (IASPEI association lecture), Union of Geodesy and Geophysics XXI General Assembly, Abstracts Week A, July 2-14, Boulder, Colorado, p. A377.

Kennett, B.L.N. and E.R. Engdahl, 1991, Travel times for global earthquake location and phase identification, *Geophys. J. Int., 105*, pp. 429-465.

Mykkeltveit, S. and H. Bungun, 1984, Processing of regional seismic events using data from small-aperture arrays, *Bull. Seis. Soc. Am., 74*, 2313-2334.

Mykkeltveit, S., F. Ringdal, T. Kvaerna and R. Alewine, 1990, Application of regional arrays in seismic verification, *Bull. Seis. Soc. Am., 80*, 1777-1800.

Vogfjord, K.S. and C.A. Langston, 1990, Analysis of regional events recorded at NORESS, *Bull. Seis. Soc. Am., 80*, 2016-2031.

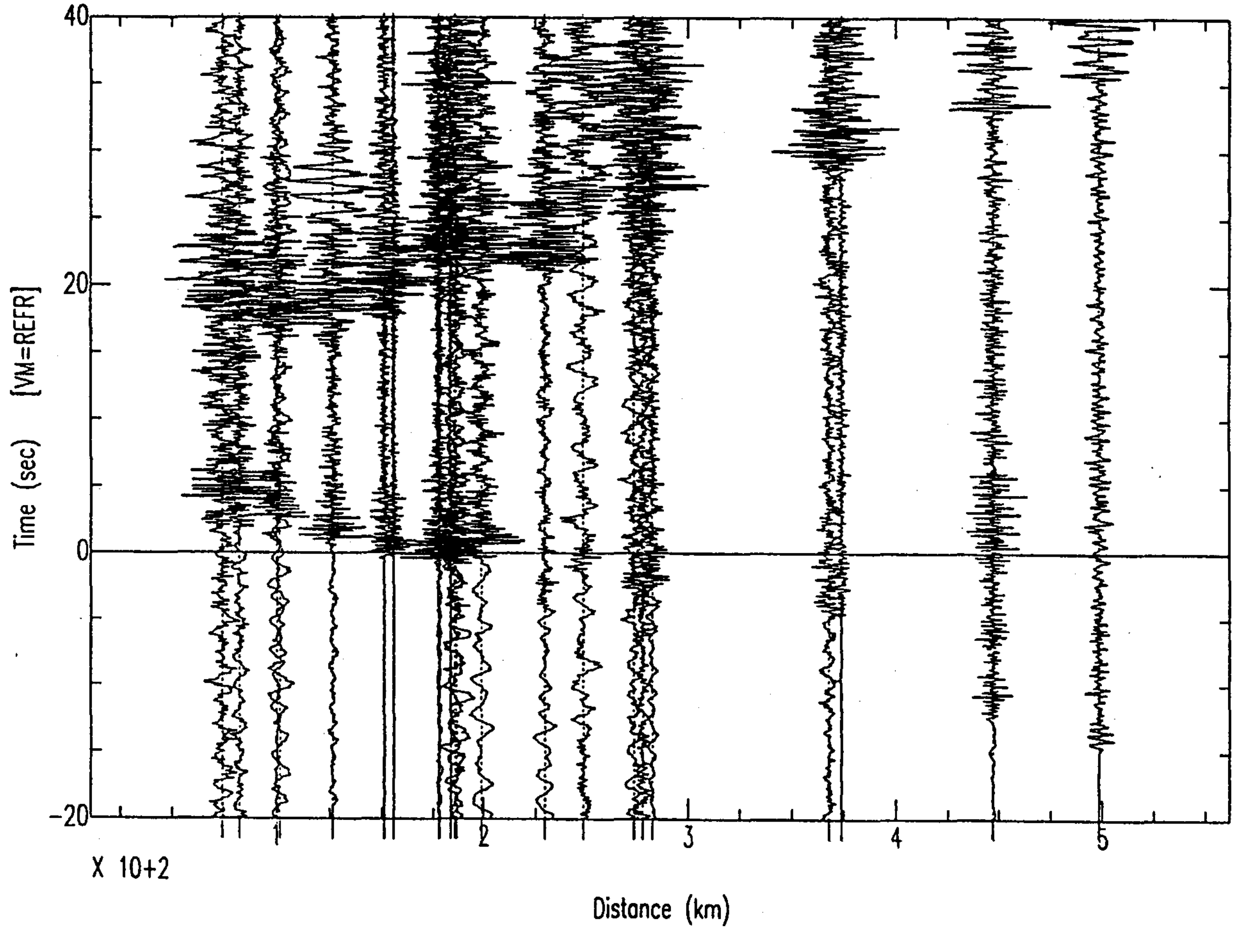

Figure 1. Regional events in record section format, distance range 0-500 km. A 6 km/sec reduction velocity has been applied.

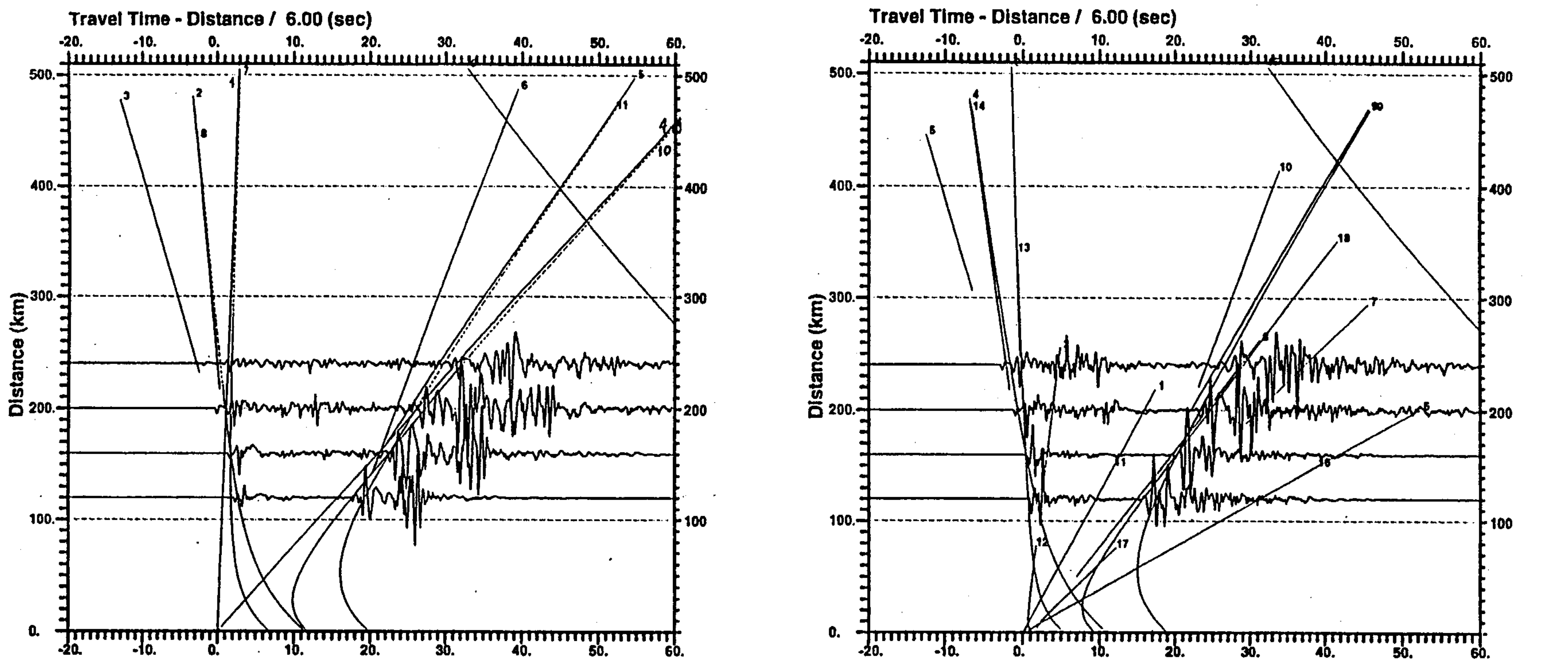

Figure 2. Linear finite difference synthetics overlain by travel time curves. Left: Model A (IASP91). Right: Model B (IASP91 with modified 4 layer crust). Travel time curves from raytracing include direct rays, refractions and reflections. For example Model A includes Pn (#3), P* (2), Pg (#1), $P_{20}P$ (#7), PmP (#8), Sn (#6), S*(#5), Sg(#4), $S_{20}S$ (#10) and SmS (#11).

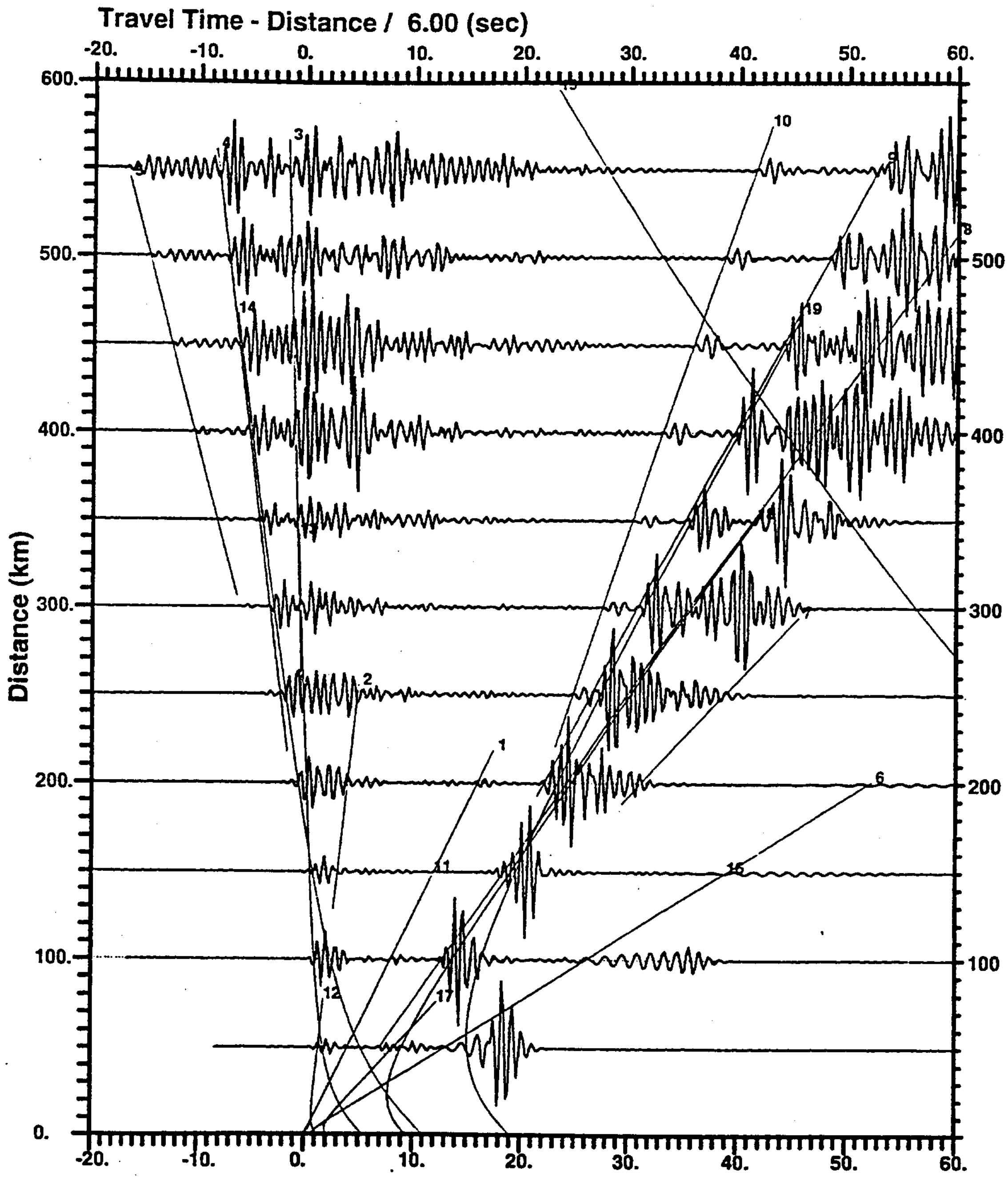

Figure 3. Reflectivity velocity synthetics overlain by travel time curves for Model B. Source is fixed at 0 km depth.

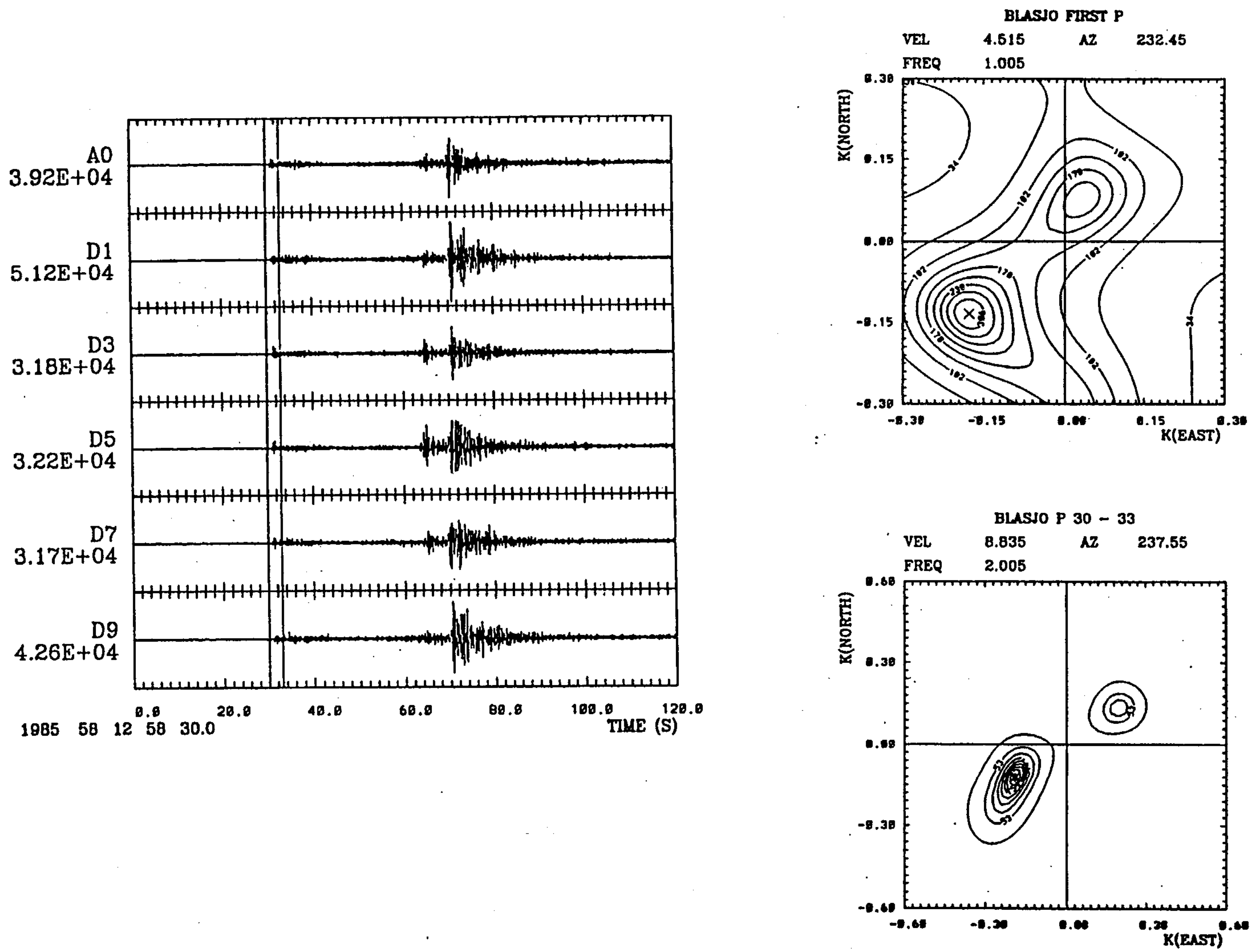

Figure 4a. NORESS recording of Blåsjø quarry blast. F-K diagrams on the right are for signal in 3 second window shown on left. Upper right: frequency band 0.9-1.1 Hz. Six stations spaced roughly 2 km apart (stations shown on left). Lower right: Frequency band 1.8-2.2 Hz. 13 stations used here (A ring, 3 from C ring, entire D ring), spaced roughly 1 km apart.

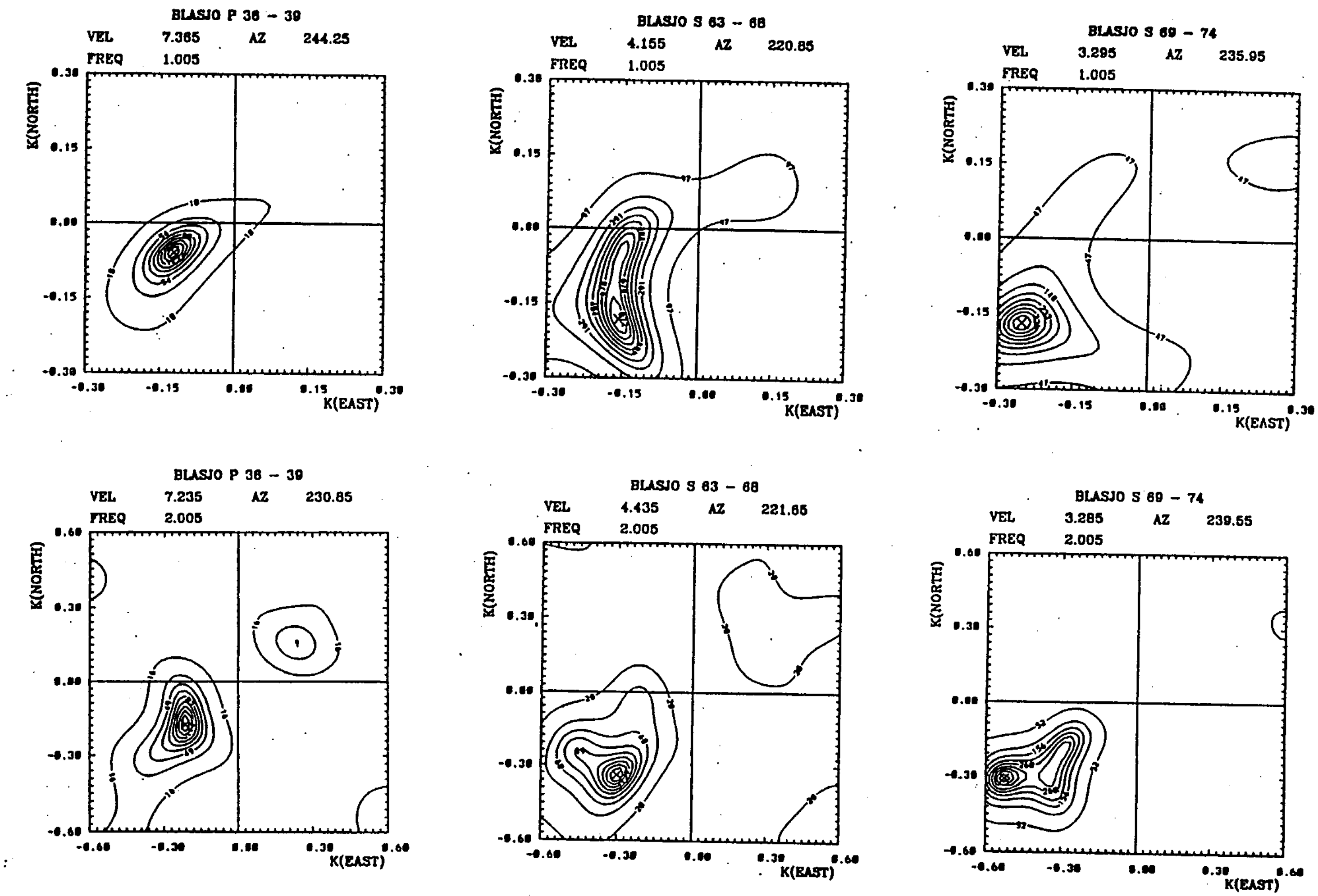

Figure 4b. Continuation of F-K plots from previous figure. Upper set of plots: 1 Hz center frequency, 6 stations. Lower set of plots: 2 Hz center frequency, 13 stations. One P and two S windows shown. Refer to Figure 4a for location of windows along seismic traces.